Ocean Engineering 100 (2015) 54–66

Contents lists available at ScienceDirect

Ocean Engineering

journal homepage: www.elsevier.com/locate/oceaneng

The performance characteristics of inclined highly pervious pipe breakwaters

Ruey-Syan Shih [a,*], Wen-Kai Weng [b], Chung-Ren Chou [b]

[a] Department of Construction and Spatial Design, Tungnan University, New Taipei City, Taiwan
[b] Department of Harbour & River Engineering, National Taiwan Ocean University, Keelung, Taiwan

ARTICLE INFO

Article history:
Received 29 December 2013
Accepted 22 March 2015

Keywords:
Inclination
Highly pervious
Pipe breakwater
Wave reflection
Wave transmission
Energy dissipation

ABSTRACT

This study investigates highly pervious dense pipes with small apertures, which benefit convection and the interchange of seawater within harbor districts and provide effective wave absorption. Additionally, this study explored the problems of wave impacts on the inclined state of highly pervious pipe obstacle, the energy dissipation characteristics for a series of inclined pipe breakwaters, and the relationship between the inclination angle and the dissipation effect. Pipe breakwaters were arranged in diverse angles of inclination. Forward inclination replicated the effects of a concave embankment, and backward inclination replicated the inclined plane of a sloping revetment. Physical experiments were conducted to investigate the influence that various apertures and inclined angles have on reflection coefficient, transmission coefficient, and loss coefficient. The results show that the influence of highly pervious inclined permeable breakwaters varies according to the effect of minimum reflectivity. The attenuation of long waves is ineffective compared to the efficacy for short waves. Lengthening the pipe enhances the effects of attenuation more compared to shifting the inclination angle, and shifting the inclination angle enhances the effects more than enlarging the aperture.

1. Introduction

Coastal protection structures, such as dense embankments and armor units, are employed to protect ports, docks, waterfronts, ecological environments, and coastal facilities from the destructive force of waves and the shore erosion. Although these structures may be effective, they may destroy the landscape and render the waterfront inaccessible. These structures are regarded as the final method for coastline protection and vary according to changes in social patterns and space requirements, thereby enhancing people's leisure activities. Because of the saturation of land leisure, the land-based leisure industry has gradually moved toward the coast. Therefore, it is necessary to consider cost effective, easy installation, environmentally friendly, and efficient landscape preserving.

Taiwan is surrounded by the ocean and has numerous large and small ports. Recently, the development of coastal leisure activities, recreation, and tourism has flourished. The geographic environments of the eastern, western, southern, and northern coasts of Taiwan are distinct. The annual seasonal winds and frequent typhoons in the summer and fall contribute to the erosion of coastal land. Walruses of many variation and considerable quantities of armor units and breakwaters have been established in coastal areas to reduce the impact that ocean waves have on land. However, these structures generally do not generally provide effective wave attenuation. Instead, they commonly cause coastal erosion and destroy the ecological environment and landscape. Numerous structures have been constructed along the coast to control wave disturbances. This has prompted extensive research of breakwaters that are comparatively inexpensive, convenient to construct and configure, environmentally friendly, and capable of providing both temporary and long term protection depending on the used type of breakwater.

In previous decades, coastal engineering researchers have investigated the physical properties and absorption of maritime structures to develop coastal defense solutions. This objective may be realized by either reflecting or dissipating approaching wave energy through induced turbulence. Safety factors, the ecological effect of the solution, effects on the landscape, and the reduction of carbon emissions generated by the leisure industry must be considered when planning coastal spaces. New types of energy dissipation structures have been extensively investigated and discussed to achieve coastal protection, prevent damage to the natural landscape, and improve the use of coastal spaces. Mani and Jayakumar (1995) designed a suspended pipe breakwater consisting of a row of closely spaced pipes mounted on a frame. The wave transmission characteristics indicate that reductions of 50% in incident wave height and 40% in investment costs can be achieved. Neelamani and Sandhya (2005) proposed dentated and serrated seawalls that reduce wave reflections by

* Corresponding author. Tel.: +886 2 86625921x157; fax: +886 2 26629583.
E-mail address: rsshih@mail.tnu.edu.tw (R.-S. Shih).

http://dx.doi.org/10.1016/j.oceaneng.2015.03.015
0029-8018/

Nomenclature

a_i	incident amplitude
a_r	reflected amplitude
D	diameter of pipes
D/h	relative pipe diameter
f	wave frequency
g	gravitational acceleration
h	water depth
h/L	water-depth wave-length ratio
H_i	incident wave height
H_r	reflected wave height
H_t	transmitted wave height
H_i/h	relative wave height
k	wave number
K_r	coefficient of reflection
K_t	coefficient of transmission
K_L	coefficient of dissipation
L	wave length
T	wave period
w	length of pipe
w/h	relative pipe length
w/L	relative ratio of pipe length to wave length
σ	angular frequency
ε	phase angle
θ	inclination angle
Δl	spacing between two probes

approximately 20–40%; thus, they are more effective for reducing wave reflections compared with plane seawalls.

Although conventional breakwaters are still employed extensively in most coastal areas, sea walls, jetties, and detached breakwaters are traditionally adopted as absorbing structures to reduce wave energy in near-shore regions. Unitary use of coastal protection structures is progressively becoming unacceptable. Today, people pay particular attention to ecological, environmental, and landscape problems. Ecological engineering methods that provide several substitutes have been developed to preserve the natural landscape and enforce the so-called amenity-oriented policy by considering energy dissipation technology, natural ecology, and landscape maintenance. The purpose of these methods is to develop coastal protection structures that are visually pleasant and provide efficient wave attenuation to mitigate coastal erosion. Modifications, such as submerged breakwaters, artificial submerged reefs, artificial beaches, amenity-oriented sea dikes, and permeable barriers, are currently preferred. Therefore, predicting how waves interact with such permeable barriers is of interest.

Investigating and designing floating breakwaters is also of great interest because these structures offer several advantages. Specifically, they can be constructed rapidly, are environmentally friendly, do not require silting or scouring, are inexpensive (which benefits regions that can afford only low capital expenditure), and can be applied for temporary protection in deep offshore areas.

However, before considering geometric configurations that facilitate wave attenuation, the stability of offshore structures must be investigated. Thus, the force in floating moorings was also examined. A wide variety of floating breakwaters, such as anchored porous breakwaters, have been designed to attenuate wave energy and reduce mooring forces. Hegde et al. (2008, 2011) subjected breakwater models composed of 3 layers to various degrees of wave steepness, width, and spacing to investigate the mooring forces of horizontally interlaced, multilayered, and floating pipe breakwaters. Their research showed that the force in seaward side moorings increases as the wave steepness increases, and decreases as the relative width increases.

Various types of inclined structures designed to reduce the impact of incoming waves and the effects of wave-structure interaction have been discussed. Previous studies have shown that inclined structures may not necessarily be more efficient compared with vertical structures, and some even report greater impact pressures and run-ups on inclined walls compared with vertical seawalls, and that the relative pressure exerted on sloping walls is slightly higher. Kirkgöz (1995) analyzed the results of an experiment concerning the impact pressures of waves breaking directly on vertical and sloping walls and found that the highest dimensional maximum impact pressure occurred on a 30° backward inclined wall, whereas the highest values of the bottom impact pressure occurred on a vertical wall. Neelamani and Muni Reddy (2002) investigated the wave forces on a vertical cylinder protected by perforated vertical and inclined barriers. Their results showed that a vertical perforated barrier is more effective for reducing wave force compared with a sloping (inclined) barrier of the same porosity. Sundar and Anand (2010) investigated variations in the run-up of vertical and curved seawalls, and found that the curvature of the Galveston seawall inadequately directs wave run-ups, increasing the run-up by approximately 25% compared with that of a vertical wall.

However, in several circumstances, inclined structures are preferred over vertical structures. Rao et al. (2009a, 2009b) examined the wave transmission of a submerged inclined plate breakwater oriented at varying inclinations. Their results indicated that inclined plate breakwaters are more effective than horizontal structures, and a plate oriented at an inclination of 60° is effective for the entire range of wave parameters and reduces wave height by 40%. Neelamani and Sandhya (2005) demonstrated that slope structures can effectively dissipate energy. Incident wave energies are dissipated because of the phase lag of reflected waves, which occurs when waves break on an inclined slope. Nakamura et al. (2001) presented a double-walled breakwater in which an inclined plate array served as the front wall. They confirmed that this structure is highly effective for reducing both reflected and transmitted waves. They also reported that the downslope model of the plate array front wall provides greater dissipation of long waves than of short waves. Koraim and Salem (2012) examined the hydrodynamic performance of a new type of breakwater consisting of half pipes suspended on supporting piles. The proposed breakwater (comprising horizontal half pipes, an increased pipe diameter, 45° inclination angle, and comparatively long drafts and wavelengths) yielded an improved performance compared with that of other types. Bayram (2000) evaluated the performance of an inclined pontoon breakwater and discussed the effects that incident wave height, wave steepness, and mooring cable length exert on the transmission coefficient with and without bottom clearance. The results showed that the inclined float breakwater is suited to shallow and intermediate water depths. The transmission decreased in accordance with increases in the wave period and mooring length, which marginally depend on the length of the structure. Murakami et al. (1994) discussed the feasibility of using breakwaters with a gradual upward- and downward-sloping plate for wave absorption, suggesting that upward-inclined plates are effective for controlling both wave absorption and water purification. Examining the performance of a submerged and horizontal plate for offshore wave control, Yu (2002) indicated that overtopping may occur on an inclined plate, but variations in plate inclination do not substantially affect the reflection and transmission. In addition, the study assessed the effects of plate length, submergence, porosity, and inclination.

According to the investigation of Koftis and Prinos (2005) regarding the hydrodynamic efficiency of 3 types of floating breakwaters (box, catamaran, and trapezoid), the performance of breakwaters is correlated to wave-structure hydrodynamics. The velocity at the edges of the structure, associated turbulence, and wave run-up and run-down on the seaward inclined face are particularly significant.

Based on wave attenuation and mooring force debasement, Wang and Sun (2010a, 2010b) examined the characteristics of geometric configurations by developing an innovative floating breakwater using numerous diamond-shaped blocks. Their results indicated that the floating breakwater reduced the height and mooring force of transmitted waves by dissipating rather than reflecting wave energy.

In this study, an inclined highly pervious pipe breakwater in a wave flume was experimentally tested to increase wave attenuation and reduce destruction caused by the force of waves. Shih (2012) investigated the performance and effectiveness of a highly pervious, perpendicularly arranged pipe breakwater. The surface of protection embankments was laid with PVC pipes to reduce the reflection area and provide high porosity and permeability, and is pervious to light. Hence, the present pipe breakwater can satisfy the following requirement: including cost effective, easy installation, environmentally friendly, and efficient landscape preserving. In addition, high pervious pipes (with low shielding rate) decrease the force exerted by the waves on the structure, and substantial reduction in wave force contributes directly to reduction in the cost of construction of the breakwater.

Wave energy was dissipated by destroying the customary particle trajectory and flow of water through the hole of the pipe. Pipe breakwaters primarily dissipate, but also partly reflect and transmit, wave energy. Forward inclination replicated the effects of a porous curved seawall (or wave return wall), and backward inclination replicated the inclined plane of a porous sloping revetment. In this study, the permeable bottom and sloping surface of a highly pervious pipe breakwater was used to reduce the wave impact force (air was not trapped and could escape easily without compression and impact pressure). The inclined surface also generated passivation effects on the sloping seawall, and the friction between the pipe hole and inclined surface affects energy dissipation and reduces the wave run-up height.

2. Experimental setup

2.1. Wave flume and generator

Physical experimental testing was conducted in a 21-m wave flume at the Fluid Mechanics Laboratory of Tungnan University. Details of wave flume and physical experimental setup, including distance between model and the wave gages were determined in Fig. 1. The flume had tempered glass on one side to facilitate observation. The channel was 0.8 m wide, 0.6 m high and the constant water depth was 25 cm. A piston-type wave generator was located at one end of the flume. At the other end was an absorbing 1:2.5 slope with 4 porous thin steel plates. The wave generator filter unit, produced by the Canadian Hydraulics Center, controlled the wave generator system. The optimal performance for wave generation was $T=0.35$ to 1.5 s, and $H=1-7$ cm; T and H denote the generated wave period and wave height, respectively. The maximum stroke distance of the piston is 50 cm, and the driving motor of the wave generator is 2 kW, 2000 r/min.

2.2. Wave gauge

The performance of the inclined highly pervious pipe breakwater was tested using regular waves to assess the efficiency and validate the design concept. Waves were measured using 5 capacitance wave gauges with an adapter linked to a personal computer. Calibration of the wave probes was performed every time at the beginning of the experiments, ensuring the accuracy of the measurements. The sampling frequency of the wave gauges is 20 Hz. The first gauge measured the incident wave heights, the second and third gauges measured the reflection coefficient, and the fourth and fifth gauges were used to estimate the transmission. The breakwater was installed in the middle of the tank, 10 m from the generator.

2.3. Model scale

A scale of 1:50 was chosen for the selection of the model dimensions in this study, the conditions carried out in the laboratory (water depth h, pipe diameter D, and wave periods T) corresponded to 12 m water depth, 0.3–0.75 m pipe diameter, and 3.5–10.6 s wave period in the prototype, respectively.

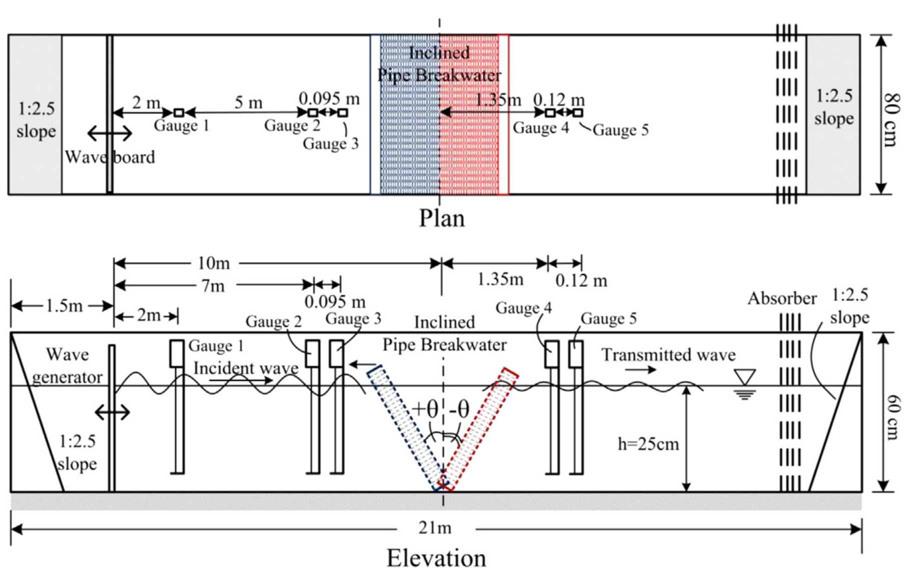

Fig. 1. Details of wave flume and physical experimental setup.

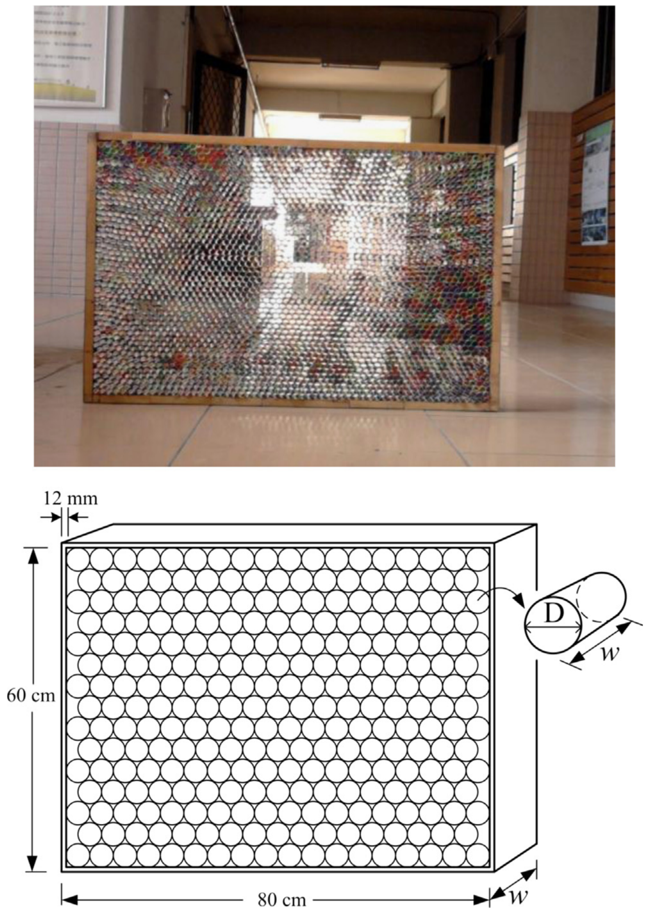

Fig. 2. Portrait and diagram sketch of pipe breakwaters.

Table 1
Shielding rate and porosity per unit area of the pipe breakwaters.

Diameter (mm), D	Shielding rate per unit area (%)	Porosity per unit area (%)
6	8.95	91.05
8	6.6	93.4
10	5.34	94.66
12	4.5	95.5
16	3.4	96.6

Table 2
Relevant physical characteristic between the present wave conditions. (Incident wave heights $H_i=1$, 2, 3, and 4 cm, water depth $h=0.25$ m).

Wave period, T (s)	Wave length, L (m)	Wave number, k (1/m)	Wave celerity, c (m/s)	h/L
Deep water wave				
0.5	0.390	16.124	0.779	0.641
Transitional water wave				
0.6	0.558	11.270	0.929	0.448
0.7	0.742	8.464	1.061	0.337
0.8	0.932	6.742	1.165	0.268
0.9	1.119	5.613	1.244	0.223
1.0	1.303	4.822	1.303	0.192
1.1	1.482	4.238	1.348	0.169
1.2	1.659	3.788	1.382	0.151
1.3	1.832	3.430	1.409	0.136
1.4	2.003	3.187	1.431	0.125
1.5	2.172	2.893	1.448	0.115
Shallow water wave				

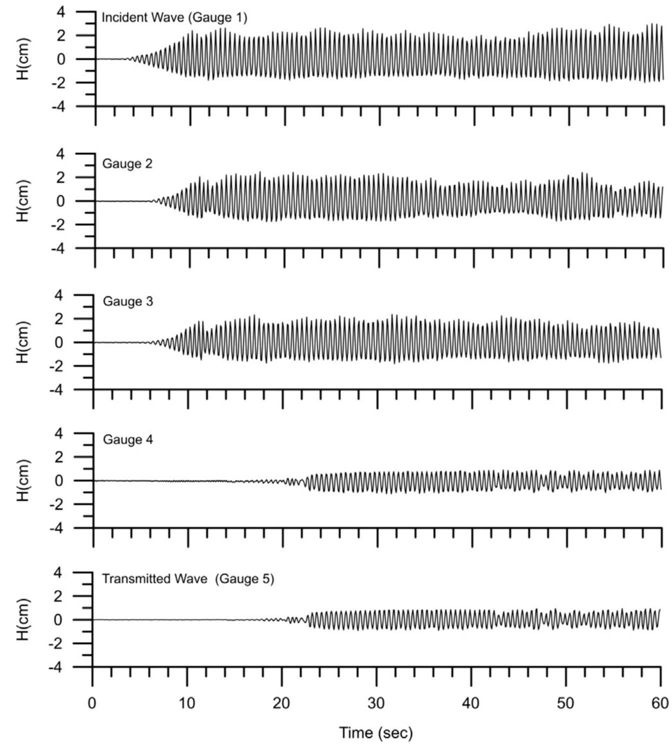

Fig. 3. Variation of waveform of incident and transmitted waves. ($T=0.5$ s, $\theta=-60°$, $D/h=0.024$, $w/h=0.2$, and $H/h=0.16$).

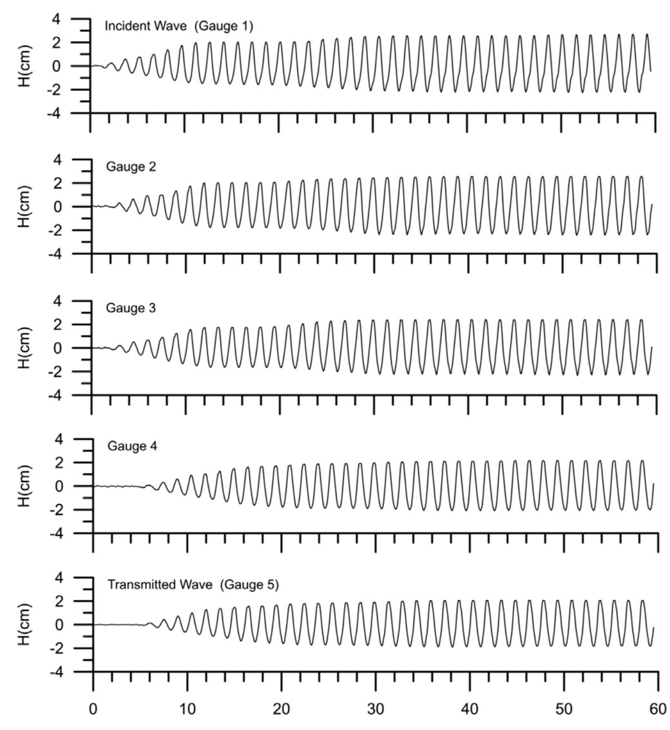

Fig. 4. Variation of waveform of incident and transmitted waves. ($T=1.5$ s, $\theta=-60°$, $D/h=0.024$, $w/h=0.2$, and $H/h=0.16$).

2.4. Model details

The pipe breakwaters were modeled using 12-mm-thick plywood and fixed into a rigid 80 cm × 60 cm frame. The frames were filled with polyvinyl chloride (PVC) pipes of various diameters D ranging from 6 mm to 15 mm ($D/h=0.024$–0.064). The length w of the longitudinal pipes (e.g., $w=5$ cm and 10 cm; $w/h=0.2$ and 0.4) (Fig. 2). The pipes were placed parallel to each other, packed tightly, and fastened. Fig. 2 shows that the translucent surface of the structure facilitates landscape maintenance and the exchange of water. In practical applications, the pipe breakwater can be conveniently cast as a module in a commercial foundry. Based on a pipe thickness of approximately 0.17 −0.18 mm, it was possible to determine the area of the model (80 cm × 60 cm) and assess the shielding rate and porosity per unit area. The results (Table 1) confirm that the model was a highly pervious structure. The pipes were placed longitudinally and parallel to the direction of incoming waves, and the breakwater was inclined. The inclination angles of the structures were $+30^\circ$ and $+60^\circ$ (denotes the forward inclination) and -30° and -60° (denotes the backward inclination), respectively. The designed pipe breakwater is higher than the water surface to prevent wave over topping.

In this study, the performance characteristics of inclined stationary pipe breakwaters were analyzed by applying incident wave heights of $H_i=1$ cm, 2 cm, 3 cm, and 4 cm ($H_i/h=0.04$–0.16) for the period ranging from $T=0.5$ s to 1.5 s. Relevant physical characteristic between the present wave conditions are listed in Table 2, which illustrates and compares the relevant physical characteristics of these conditions, including wave lengths and h/L parameters, where h/L varied from 0.115 to 0.641. The waves within the ambit were classified as deep water wave ($T=0.5$ s), transitional water waves ($T=0.6-1.5$ s), and contains most of the nearshore wave range.

3. Estimation of wave attenuation

Waves were measured using five capacitance wave gauges (Fig. 1) with an adapter linked to a personal computer. An absorbing slope was employed in the end of flume to reduce reflected waves, however, a quantity of reflected wave reflect from the 1:2.5 slope and absorbing thin porous plate inevitably contaminate the incident wave train. The distance of wave gages was set to minimize the influence of re-reflected waves from the generator according to the 21-m wave flume. The locations of gauges from both the structure and wave paddle for wave resolution are selected according to the recommendation of Goda and Suzuki (1976). The incident wave height H_i was calculated by analyzing the water elevation measured by the first gauge, individual waves have been delineated by zero-up crossing method. The reflection and transmission of wave energy were

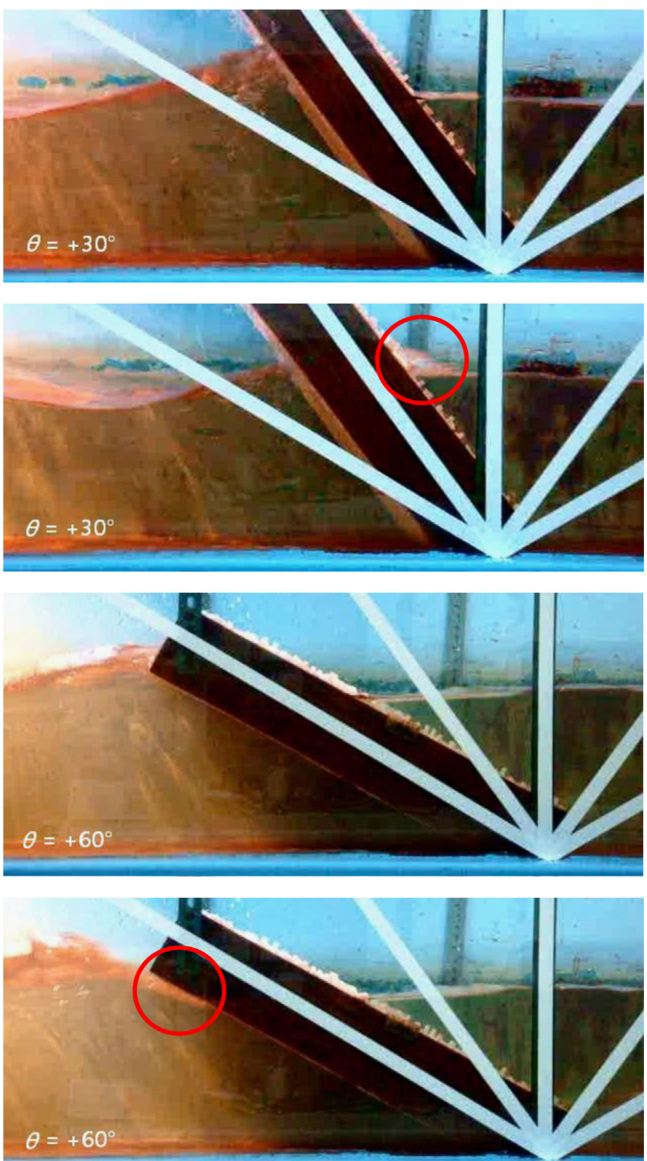

Fig. 5. Impact of the waves against the forward-inclined pipe breakwater ($D/h=0.024$, $w/h=0.4$, $\theta=+30^\circ$ and $+60^\circ$).

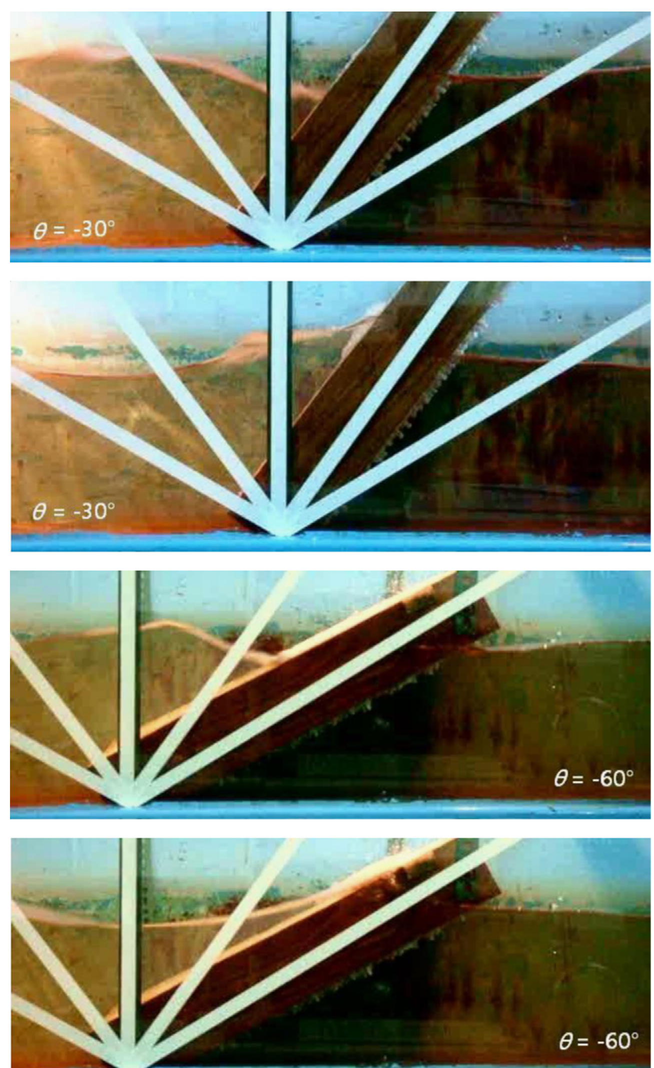

Fig. 6. Impact of the waves against the backward-inclined pipe breakwater ($D/h=0.024$, $w/h=0.4$, $\theta=-30^\circ$ and -60°).

estimated using the well-known method established by Goda and Suzuki (1976) for separating the incident and reflected waves. Based on the time histories of water elevations measured using 2 wave gauges (Gauge 2 and Gauge 3) on the free water surface, the distance between the gauges is 0.095 m, the amplitudes were analyzed using the Fast Fourier Transform (FFT) technique. Thus, the reflection coefficients K_r were estimated as follows:

The composite wave profiles of incident and reflected waves at location $x=x_1$ and $x=x_1+\Delta l$ can be expressed as

$$\eta_1=(\eta_i+\eta_r)_{x=x1}=A_1 \cos \sigma t+B_1 \sin \sigma t \tag{1}$$

$$\begin{cases} A_1=a_i \cos \theta_i+a_r \cos \theta_r \\ B_1=a_i \sin \theta_i+a_r \sin \theta_r \end{cases} \tag{2}$$

$$\eta_2=(\eta_i+\eta_r)_{x=x1+\Delta l}=A_2 \cos \sigma t+B_2 \sin \sigma t \tag{3}$$

$$\begin{cases} A_2=a_i \cos(\theta_i+k\Delta l)+a_r \cos(\theta_r+k\Delta l) \\ B_2=a_i \sin(\theta_i+k\Delta l)+a_r \sin(\theta_r+k\Delta l) \end{cases} \tag{4}$$

where $\theta_i=kx_1+\varepsilon_i$, $\theta_r=kx_1+\varepsilon_r$, k is the wave number, σ is the angular frequency, and ε is the phase angle. Subscripts "i" and "r" denote incident and reflected waves, respectively. Finally, Δl represents the spacing between 2 measuring stations.

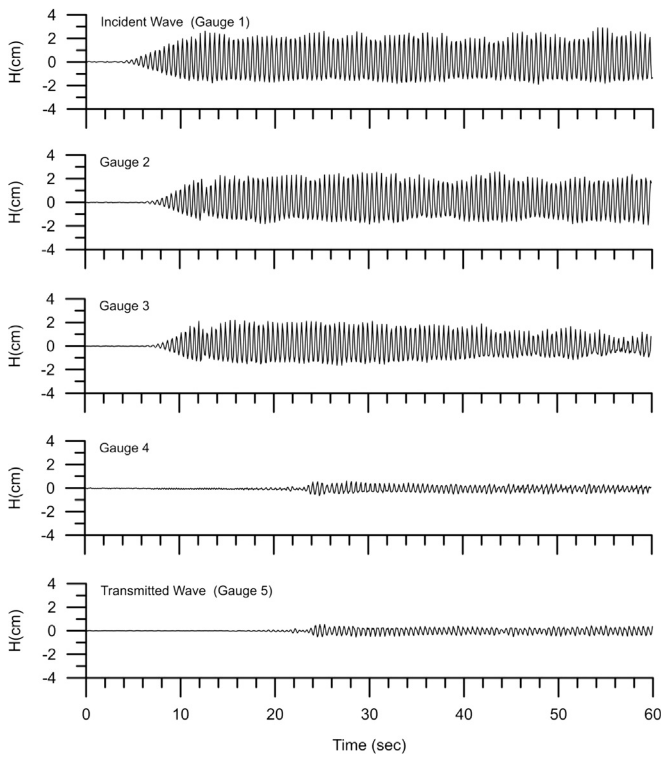

Fig. 7. Variation of waveform of incident and transmitted waves ($T=0.5$ s, $\theta=+60°$, $D/h=0.024$, $w/h=0.2$, and $H/h=0.16$).

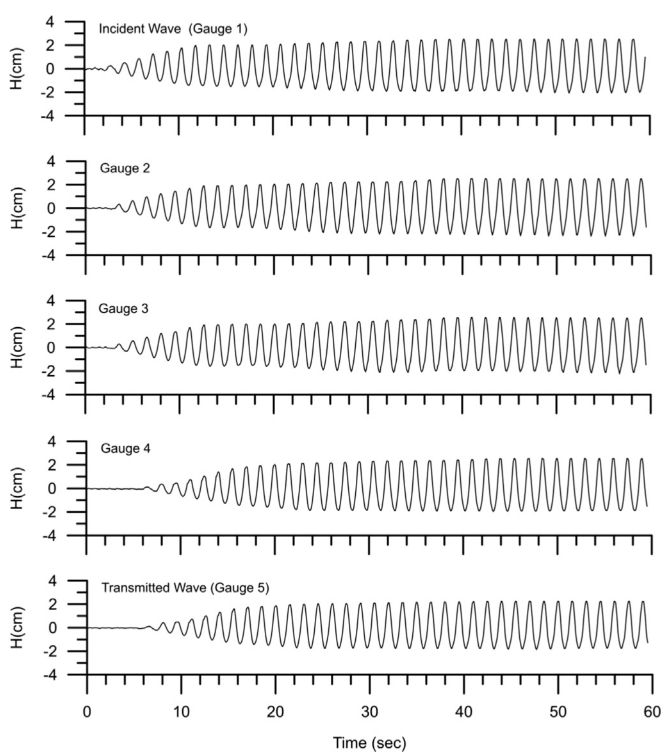

Fig. 8. Variation of waveform of incident and transmitted waves ($T=1.5$ s, $\theta=+60°$, $D/h=0.024$, $w/h=0.2$, and $H/h=0.16$).

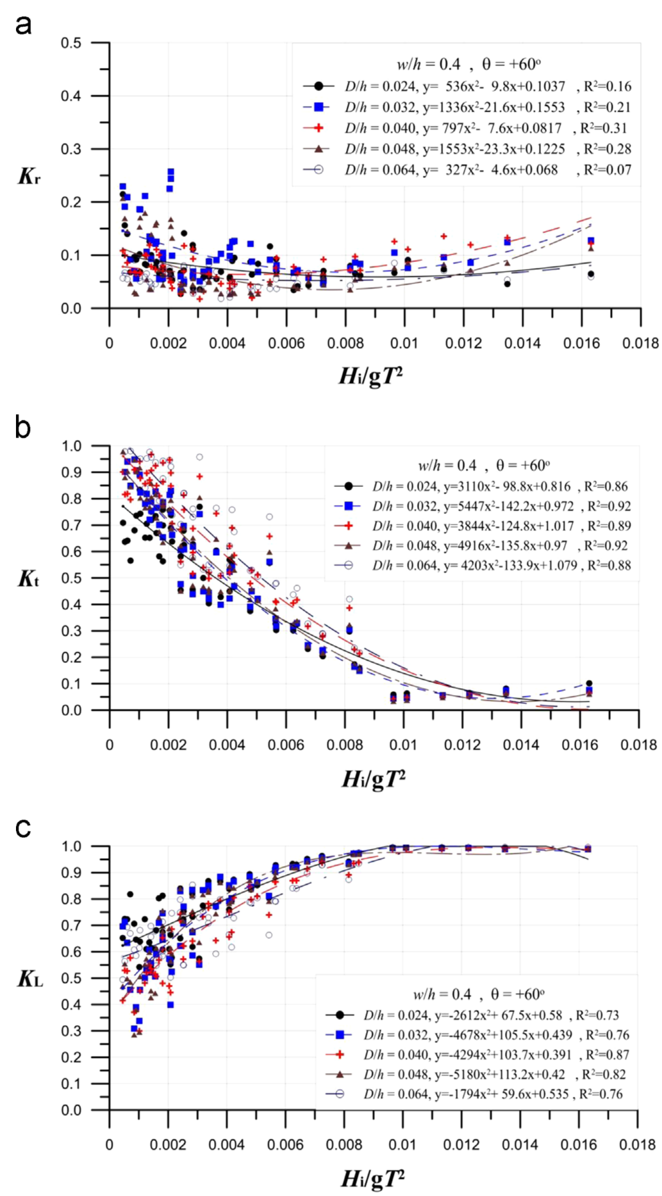

Fig. 9. Diversity of K_r, K_t, and K_L relative to pipe diameter at $w/h=0.4$ and $\theta=+60°$.

Therefore, amplitudes a_i and a_r can be calculated as follows:

$$a_i = \frac{1}{2|\sin k\Delta l|}[(A_2 - A_1 \cos k\Delta l - B_1 \sin k\Delta l)^2 + (B_2 + A_1 \sin k\Delta l - B_1 \cos k\Delta l)^2]^{1/2} \quad (5)$$

$$a_r = \frac{1}{2|\sin k\Delta l|}[(A_2 - A_1 \cos k\Delta l + B_1 \sin k\Delta l)^2 + (B_2 - A_1 \sin k\Delta l - B_1 \cos k\Delta l)^2]^{1/2} \quad (6)$$

The reflection coefficient K_r can be obtained using

$$K_r = \frac{H_r}{H_i} \quad (9)$$

The wave transmission coefficients K_t were estimated using

$$K_t = \frac{H_t}{H_i} \quad (10)$$

where H_i, H_r, and H_t denote the incident wave height, reflected wave height, and transmitted wave height, respectively.

Consequently, according to Reddy and Neelamani (1992), wave attenuation (loss coefficient, K_L) can be estimated as

$$K_L = \sqrt{1 - K_r^2 - K_t^2} \quad (11)$$

4. Results and discussion

The analysis presents the efficiency of the breakwater in the form of relationships between transmission, reflection, and energy dissipation coefficients (K_t, K_r, K_L) and dimensionless parameters. These parameters represent the wave and structure characteristics as given in the following equation:

$$K_t, K_r, K_L = f(H_i/gT^2, D/h, w/h, H_i/h, \theta, h/L) \quad (12)$$

4.1. Waveform variation

Fig. 3 shows the variations in the waveforms of all wave gages when T=0.5 s, and 1.5 s at $\theta = -60°$, D/h=0.024, w/h=0.2, and H_i/h=0.16. The transmission was considerably reduced when T=0.5 s because of the relatively small aperture and short wavelength, which limited the wave heights. When T=1.5 s, the wave length exceeded that at T=0.5 s, with only slightly decline in wave height (Fig.4). Fig. 5 shows the impact of the waves against the forward-inclined pipe breakwater when D/h=0.024, w/h=0.4 at $\theta = +30°$ and $+60°$, the incident waves were apparently dissipated, air bubbles occurs behind the breakwaters when waves transmitted through the pipes. As shown in Fig. 5, the forward inclination case behave as a curved-seawall, when the inclination angle is greater (e.g., 60°), the pipes within the structure is relatively steep (vertically), the fluid rushed up through the structure, but then fell in the wave-front side of the structure. When the angle is 30°, as shown in the second figure, broken waves occurred as the waves propagated through the structure. The impact of the waves against the backward-inclined pipe breakwater at $\theta = -30°$ and $-60°$ was shown in Fig. 6, waves run-up on the sloping surface replicating inclined plane of a

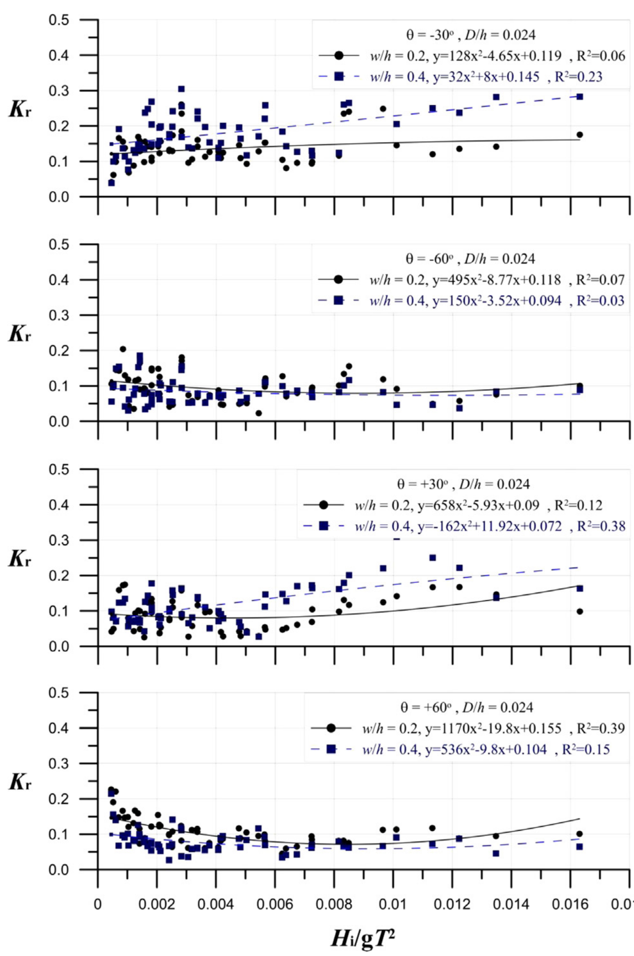

Fig. 10. Variation of reflection coefficient K_r versus H_i/gT^2 at w/h=0.2 and 0.4 when D/h=0.024.

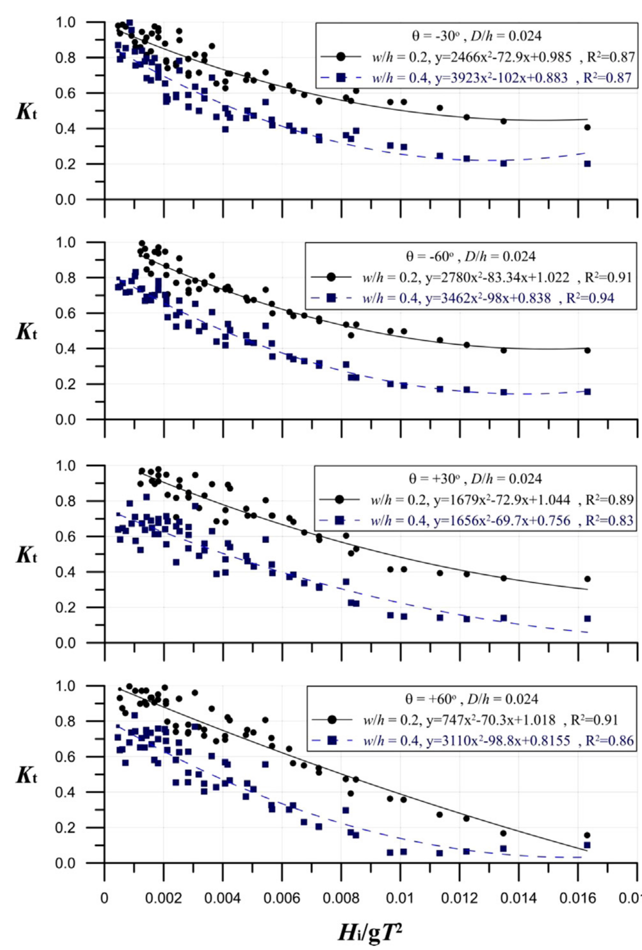

Fig. 11. Variation of transmission coefficient K_t versus H_i/gT^2 at w/h=0.2 and 0.4 when D/h=0.024.

sloping revetment, however, the plane were filled with highly pervious dense pipes, water are mostly permeated (through the pipes). Fig. 6 showed the backward inclination case, which behave as a permeable sloping bottom, however, though the wave run-up along the surface of the pipe breakwater, no breaking wave occurred. The dissipation of wave energy may due to the vortex instead of surf beat; this argument requires further study and validation.

Fig. 7 shows the waveforms variations of all five wave gages applied when the inclination angle $\theta=+60^{\circ}$ and the pipe length $w/h=0.2$. Here, the transmitted wave height was less than that when $\theta=-60^{\circ}$ and $T=0.5$ s. The waveforms of the transmitted waves were similar to that at $T=1.5$ s (Fig. 8). This indicates that varying the inclination angle from backward ($\theta=-60^{\circ}$) to forward ($\theta=+60^{\circ}$) exerted no apparent effect on long waves; instead, the energy dissipation of short waves was more affected.

4.2. Characteristics of energy dissipation

The experiments were conducted under the condition of non-breaking waves to observe variations in the reflection coefficient K_r, transmission coefficient K_t, and loss coefficient K_L when a wave passed through the inclined highly pervious pipe breakwater. The following sections provide a comprehensive discussion and analysis of the results obtained when the diameters, lengths, and inclination angles of the pipes, as well as the incident wave heights and wave periods, were varied. The variations of K_t, K_r and K_L are discussed by using polynomial curve fitting,

4.2.1. Effect of pipe apertures on K_r, K_t, and K_L

As shown in Fig. 9a, the diversity variation of K_r in relation to the pipe diameter D/h indicates that the reflection decreased initially, but then increased when H_i/gT^2 increased. Minimum variation occurred near $H_i/gT^2=0.008$, the overall tendency of the variation in reflection was similar to that under varied D/h due to their close value of shielding rate and porosity per unit area, but the variation in curvature was comparatively greater when $D/h=0.064$, and the curvature varied minimally when $D/h=0.024$.

When $w/h=0.4$, $\theta=+60^{\circ}$, and $D/h=0.024$, the transmission coefficient K_t ranged between 0.6 and 0.8 when the wavelength was comparatively long (i.e., $H_i/gT^2=0.00045-0.002$). When the pipe diameter D/h was increased to 0.064, the K_t values raised up between 0.8 and 0.95, indicating that the K_t values increased as the aperture increased (Fig. 9b). As shown in the Figure, the transmission coefficient K_t decreased when H_i/gT^2 increased. Almost no transmitted waves existed in short-period waves, except when $H_i/gT^2<0.004$, the remainder of K_t was less than 0.5. When $H_i/gT^2>0.012$, K_t was less than 0.1. The same tendency appeared when alternative diameters were applied. By contrast, a minimum K_t value exists at $D/h=0.024$, and was relatively larger when $D/h=0.064$.

When D/h remained identical, the variation of the loss coefficient K_L increased initially before decreasing slightly when H_i/gT^2 was increased (Fig. 9c). When $H_i/gT^2=0.01$, a relatively large value was recorded and the curve of $D/h=0.024$ was higher than other curves. The curve of $D/h=0.064$ was the lowest curve. Thus, the attenuation of $D/h=0.024$ was superior to that of $D/h=0.064$.

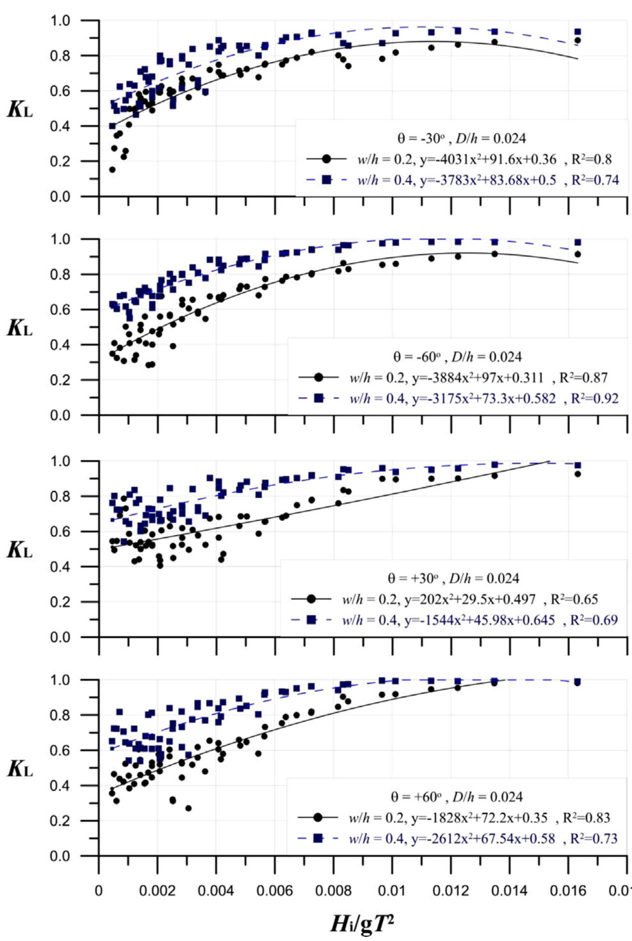

Fig. 12. Variation of loss coefficient K_L versus H_i/gT^2 at $w/h=0.2$ and 0.4 when $D/h=0.024$.

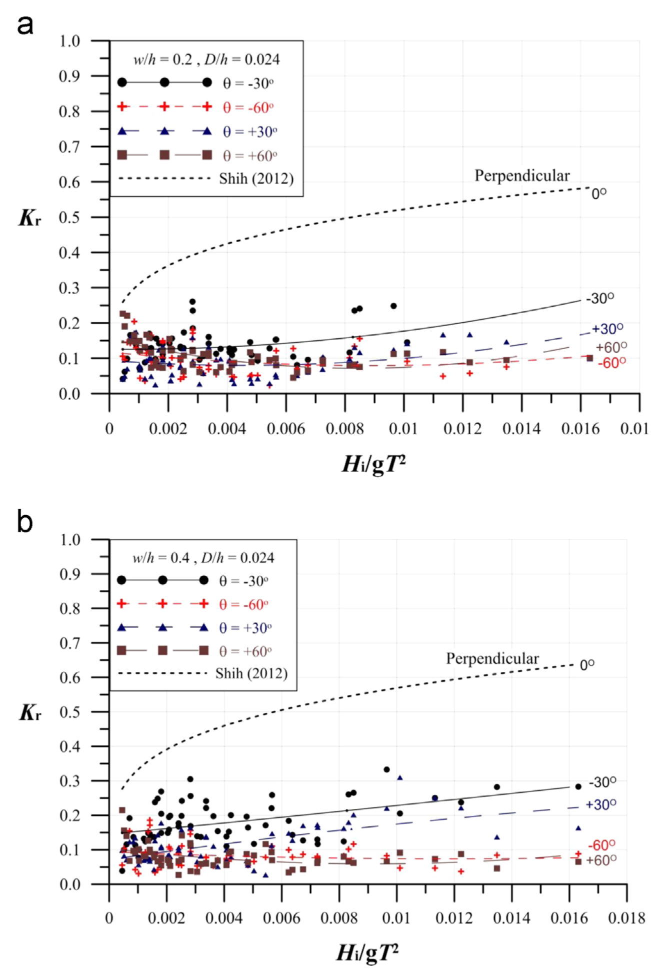

Fig. 13. Variation of loss coefficient K_L versus H_i/gT^2 at various inclination. ($D/h=0.024$, $w/h=0.2$ and 0.4).

In summary, when using a small pipe diameter, the reflection and transmission were relatively low, whereas the loss coefficient was relatively high. However, little variability and limited impact was found, indicating varying the pipe diameter exerted a limited effect on the results.

4.2.2. *Effect of pipe length on K_r, K_t, and K_L*

Figs. 10–12 showed the effect of pipe length on the reflection, transmission, and energy dissipation. The reflection coefficient K_r ranged between 0.05 and 0.15 when $D/h=0.024$, $\theta=+60^\circ$, and $w/h=0.2$. When the pipe was lengthened to $w/h=0.4$, the reflection coefficient decreased to 0.05–0.1. Similarly, when $\theta=-60^\circ$, the reflection coefficient K_r ranged between 0.05 and 0.1 when $w/h=0.2$, the values are almost similar when increasing w/h to 0.4. K_r initially reduced and then increased. The minimum value was approximately $H_i/gT^2=0.008$, variation in the corresponding K_r value decreased slightly as the pipe length was increased, the overall effect was not apparent. However, comparing the results of $w/h=0.2$ and $w/h=0.4$ when $\theta=-30^\circ$ and $+30^\circ$, K_r value increased as pipe length increased, reflection coefficient K_r ranged between 0.1 and 0.3, the overall effect was more obvious than that of larger inclination. The variation in K_r resulting from differing pipe lengths indicates that the reflection of the inclined pipe breakwater showed less discrepancy between $w/h=0.2$ and $w/h=0.4$, because the opacity of the embankment surface was similar according to Table 1.

Fig. 11 shows variations in the transmission coefficient K_t that resulted from using different pipe lengths. Unlike reflectivity, variation in transmission resulting from different pipe lengths was obvious. When $H_i/gT^2>0.004$ and $w/h=0.4$, the transmission coefficient declined more than 50% in relation to $w/h=0.2$, and both rates were less than 0.5 when $H_i/gT^2>0.008$. The overall transmission decreased as H_i/gT^2 increased. When $w/h=0.4$ and $H_i/gT^2>0.14$, K_t was reduced to less than 0.1. Almost no waves passed through the structure. The variation in the corresponding K_t value indicated that the transmission decreased significantly as the pipe length increased, and that the wave period affected the transmission evidently, they decreased as H_i/gT^2 increased.

The variation in K_L resulting from different pipe lengths indicates that dissipation increased substantially with increases in H_i/gT^2 (Fig. 12). In other words, the energy dissipation effect was more effective for short-period waves than for long-period waves. When $w/h=0.4$, the energy dissipation visibly exceeded that when $w/h=0.2$, with the highest point of the curve reaching 0.8 when $H_i/gT^2>0.004$. Under these conditions, more than 50% of the energy was dissipated.

Accordingly, pipe length had the greatest effect on K_t, followed by K_L; the effect was generally unapparent for K_r.

4.2.3. *Effect of the inclination angle on K_r, K_t, and K_L*

As shown in Fig. 13, when $D/h=0.024$, $\theta=-60^\circ$ and $+60^\circ$, no significant variation in reflectivity was observed with variations in θ. The K_r values were evenly distributed near 0.1 when $w/h=0.2$ and 0.4, varying slightly with minor discrepancies according to the variation of H_i/gT^2. Variations in K_r were maintained at approximately 0.1. No notable discrepancy was found as H_i/gT^2 increased.

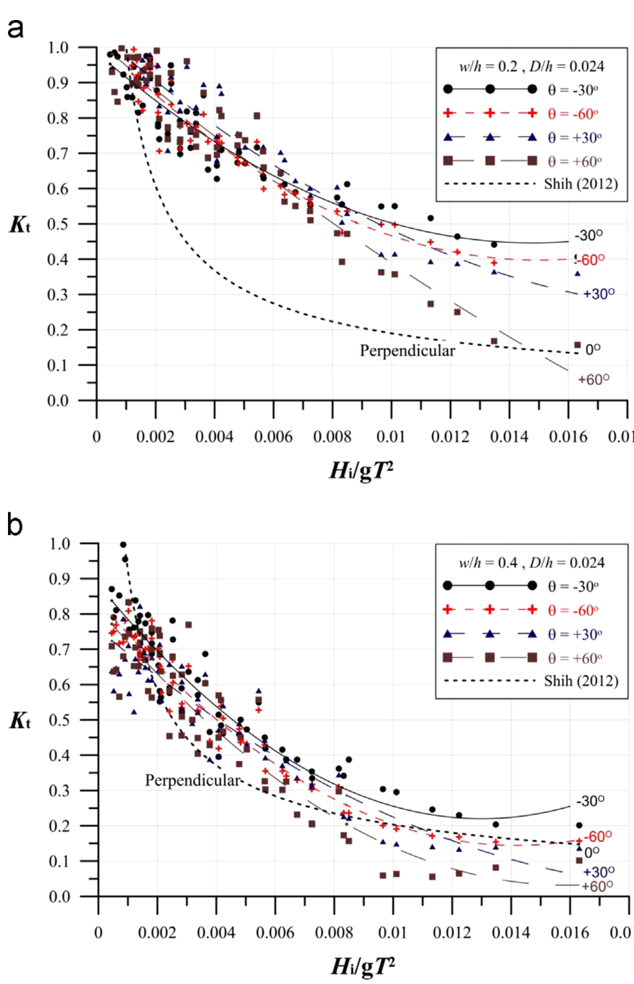

Fig. 14. Variation of transmission coefficient K_t versus H_i/gT^2 at various inclination. ($D/h=0.024$, $w/h=0.2$ and 0.4). (a) w/h=0.2, and (b) w/h=0.4.

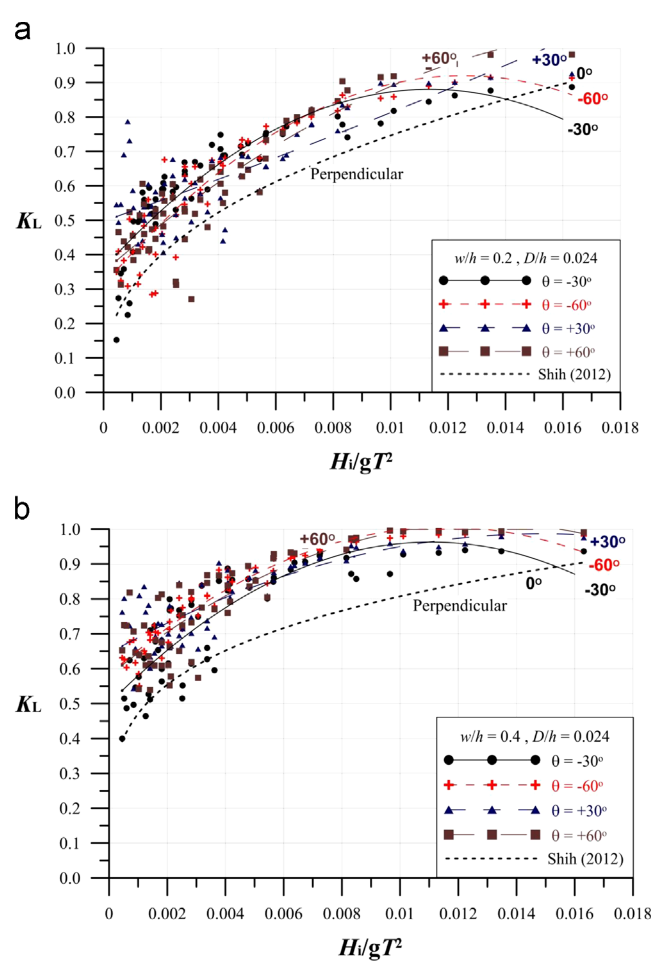

Fig. 15. Variation of loss coefficient K_L versus H_i/gT^2 at various inclination. ($D/h=0.024$, $w/h=0.2$ and 0.4).

When the incline angle is reduced to $\theta = -30°$ and $+30°$, the K_r values evenly distributed from 0.15 to 0.25 at $\theta = -30°$, other cases involving various inclination angles showed varying degrees of reflectivity effects. This indicates that the reflection coefficient increased as the inclination angle decreased from $\pm 60°$ to $\pm 30°$, a maximum value existed at $\theta = -30°$, and minimum at $\theta = +60°$. However, the variation in K_r resulting from differing pipe inclination indicates that the reflection of the breakwater showed more discrepancy between $\theta = -30°$ and $+30°$, they stabilized between 0.1 and 0.3, and decreased as the angle increased. The reflection coefficients were substantially less than that of perpendicular results by Shih (2012).

Regarding the transmission, when $D/h = 0.024$ and $w/h = 0.2$, the variation in K_t declined rapidly from 0.95 to 0.45 with the increasing of H_i/gT^2 when the inclination angle was $\theta = -30°$ (Fig. 14a). Among the other 3 conditions of inclination, where the inclination angle θ was equal to $-60°$, $+30°$, and $+60°$, the effect on transmission was greater in the forward-inclined structure (i.e. $\theta = +30°$, and $+60°$), and the greatest when $\theta = +60°$, reducing in K_t from 0.95 to 0.1. These results show that K_t decreased gradually as H_i/gT^2 increased, K_t values were less than 0.5 when $H_i/gT^2 > 0.01$. Varying the inclination angle greatly affected the variations of transmission coefficient when $H_i/gT^2 > 0.01$.

When $w/h = 0.4$ (Fig. 14b), the variation in K_t declined similarly but more intense than that in $w/h = 0.2$. The variation in K_t declined rapidly from 0.85 to 0.2 with the increasing of H_i/gT^2 when $\theta = -30°$. The largest decrease was also recorded when $\theta = +60°$, reducing in K_t from 0.85 to 0.05. These results show that K_t decreased as H_i/gT^2 increased. Therefore, the experiment results indicate that when $H_i/gT^2 >$ 0.004, the K_t values for other conditions of inclination were generally less than 0.5, all K_t values were less than 0.25 when $H_i/gT^2 > 0.01$. The transmitted coefficients were substantially larger than that of perpendicular results by

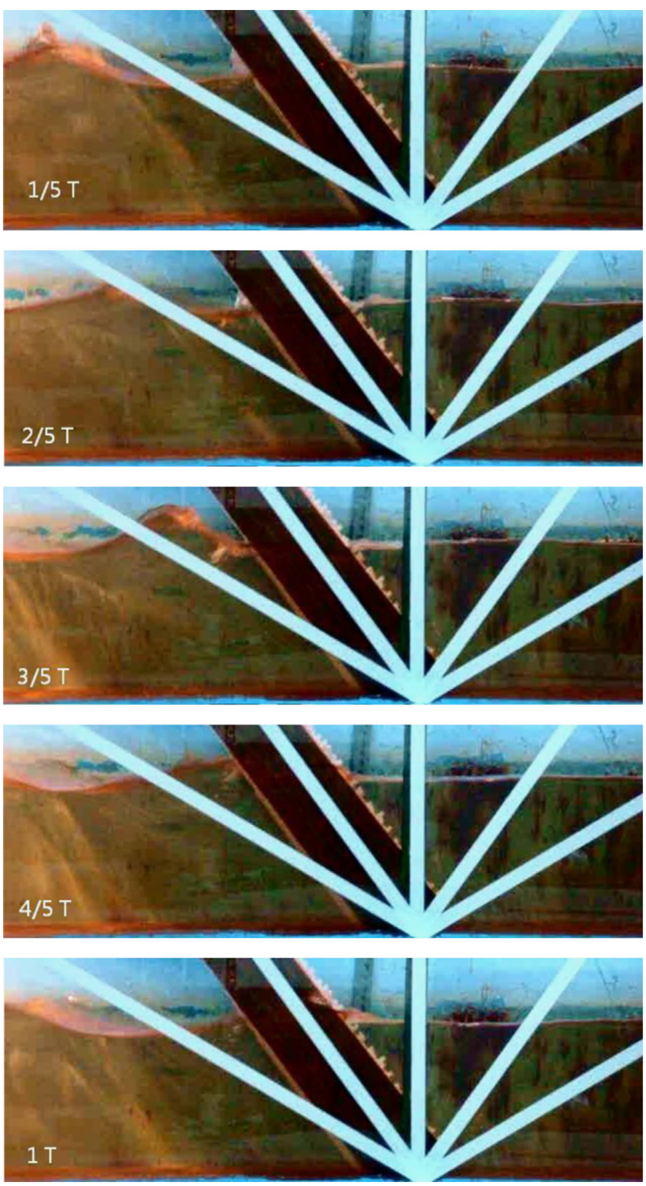

Fig. 16. Attenuation process of incident wave by forward-inclined pipe breakwater. ($D/h = 0.024$, $w/h = 0.4$, $\theta = +30°$).

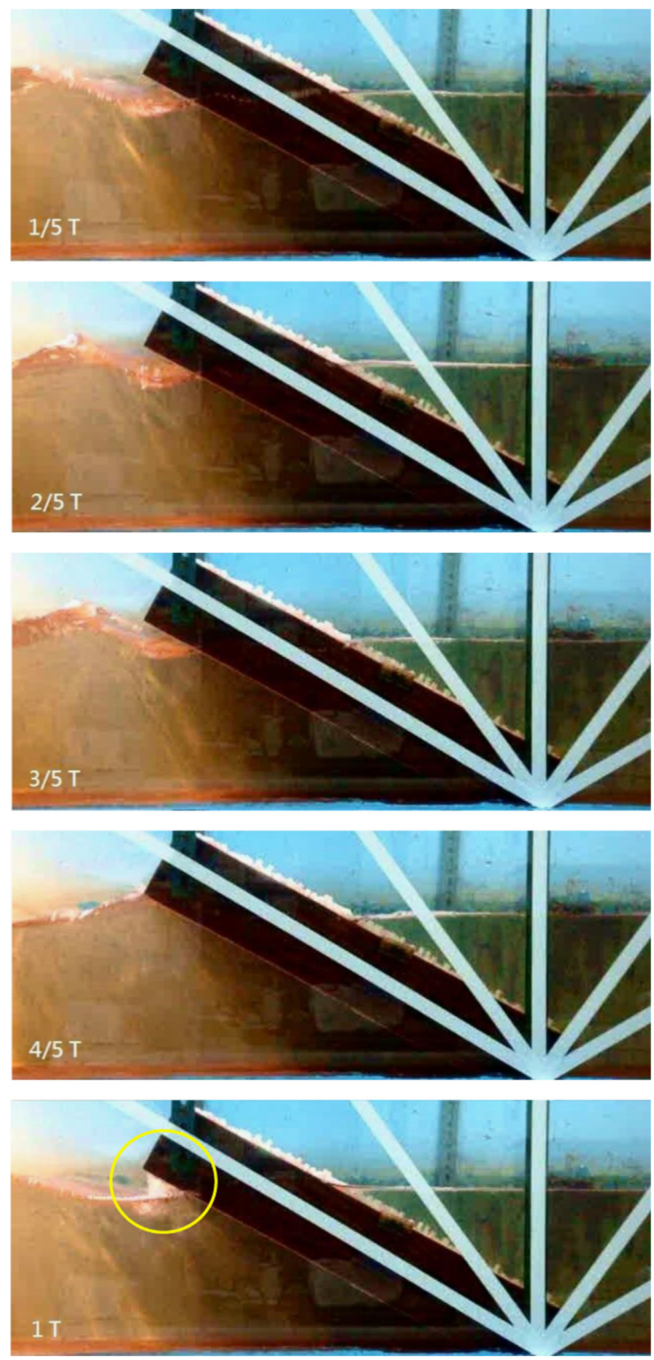

Fig. 17. Attenuation process of incident wave by forward-inclined pipe breakwater. ($D/h = 0.024$, $w/h = 0.4$, $\theta = +60°$).

Table 3
Characteristics of experimental studies of literature review.

Reference	Structure type	Studied characters	Main parameters ranges
Bergmann and Oumeraci (1998)	Permeable vertical walls	*Pressure*	P=0–45%, T=4.5–12 *s*, H_i=0.5–1.5 m, h=4 m
Rao et al. (2002)	Two rows perforated hollow piles	K_t, K_r, and K_L	H_i/gT^2=0.0006–0.008, b/D=0.5–1.0, B/D=0.5–2.0, h=0.4 m
Brossard et al. (2003)	Semi-immersed perforated wall	K_t, K_r	kh=0.9–3.0, B=0.36–0.54, i=0.08–0.16, T=0.56–1.23 s, h=0.2 m
Neelamani et al. (2006)	Single surface smooth plate	K_t, K_r, and K_L	B/h=2, b/B=0.01, D/h=0.02, h/L=0.09–0.31
Huang (2007)	Single rectangular vertical slots	K_t, K_r, and K_L	H_i/gT^2=0.003–0.012, D/h=0.46, h=0.3 m, θ=90°
Rao et al. (2009a, 2009b)	Single suspended horizontal pipes	K_L	H_i/gT^2=0.003–0.012, D/h=0.46, h=0.5 m, θ=90°
	Horizontal thin submerged plate	K_t, K_r, and K_L	H_i/gT^2=0.001–0.016, h/L=0.05–0.35, h=0.3–0.5 m
Liu et al. (2009)	Single submerged smooth plate	K_t, K_r, and K_L	B/h=2, b/B=0.02, D/h=0.37, h/L=0.21–0.42, h=0.3 m
Teh et al. (2010, 2012a, 2012b)	Composite semi-circular floating caisson	K_t, K_r, and K_L	B/h=0.714, D/h=0.071, H_i /L=0.01–0.1
Koraim and Salem (2012)	Single semi-immersed horizontal half pipes	K_t, K_r, and K_L	H_i/gT^2=0.003–0.012, D/h=0.46, h=0.2 m, θ=45°
Shih (2012)	Single immersed horizontal pipes	K_t, K_r, and K_L	H_i/gT^2=0.001–0.016, D/h=0.024–0.064, h=0.2 m
Koraim et al. (2013)	Single suspended horizontal half pipes	K_t, K_r, and K_d	B/h=1.32, B/d=10, b/B=0.05, D/h=0.07, 0.46, h/L=0.08–0.42
Patil et al. (2011, 2014)	Multi-layer horizontal floating pipe	K_t	H_i=3–18 cm, D=32 mm, w/L=0.4–2.65, T=1.2–2.2 s
Koraim et al. (2014)	Double rows horizontal piles	K_t, K_r, and K_d	H_i=0.027–0.1 m, D=0.08–0.24 m, h=0.32 m, T=1.15–2.85 s

Shih (2012) when w/h=0.2. This results have been significantly improved when w/h=0.4.

Fig. 15 shows the variation in K_L relative to pipe inclination. According to the loss coefficient for the inclined angles of the 4 configurations, the energy dissipation effect was similar, except when $H_i/gT^2>0.012$ at w/h=0.2 (Fig. 15a). The dissipation effects of the various inclinations indicate that efficiency of inclination angle had a great effect on the variation of loss coefficient K_L, but had minimum effect on their discrepancy. Among the 4 inclinations, the variation tendency of the energy dissipation coefficients was similar along the H_i/gT^2 axis, increasing considerably as H_i/gT^2 increased. The maximum K_L value was approximately between 0.85 and 0.95 at H_i/gT^2=0.012, some K_L values decreased slightly when $H_i/gT^2>0.012$, greater incidence was observed when $\theta=+60°$. Additionally, when w/h=0.4, the variation in the corresponding K_L value increased as the pipe length was increased, the overall tendency of efficiency was similar to w/h=0.2 among various inclinations. However, the loss coefficient K_L developed more than 30% in relation to w/h=0.2. Compare the results with perpendicular cases, the distributions of loss coefficients were greater than the results by Shih (2012).

The experiment results showed that maximum attenuation occurred when the breakwater was inclined forward at a wide angle. Figs. 16 and 17 showed the attenuation process of incident wave by forward-inclined pipe breakwater of $\theta=+30°$ and $+60°$ when w/h=0.4. The greatest effect occurred when the inclination angle of the pipe breakwater was $\theta=+60°$. This may be because of the increasing contact areas of the horizontal plane and the increasing resistance of the pipe structures. In the forward-inclined structure, the effect increased because the buffer space between the incoming waves and the breakwaters was reduced, this caused the waves to decline.

4.3. Comparison of hydrodynamic efficiency

Numerous of different screen breakwaters are detailed compared and analysis in Koraim et al. (2014). Important characteristics of the relevant structures are shown in Table 3. Koraim (2013) indicated that high scatter in the performance of different compared models may be attributed to the difference in the model geometry and cross sections shape. However, the variation tendency of reflection coefficient, transmission coefficient, and loss coefficient (dissipation coefficient) were analogous and significant, and corresponding with some particular parameters such as incident wave height H_i, wave length L, pipe diameter D, and breakwater width B. Figs. 18–20 showed the comparisons between the performance of present breakwater with other types of breakwaters (Koraim, 2013). As shown in Fig. 18, the present pipe

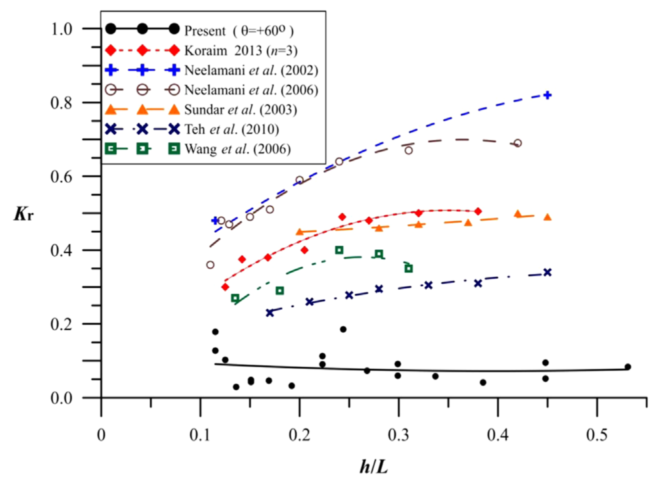

Fig. 18. Comparison of the reflection coefficient K_r between the present highly pervious pipe breakwater (D/h=0.024, w/h=0.4 and $\theta=+60°$) and different models from previous studies (Neelamani and Gayathri, 2006).

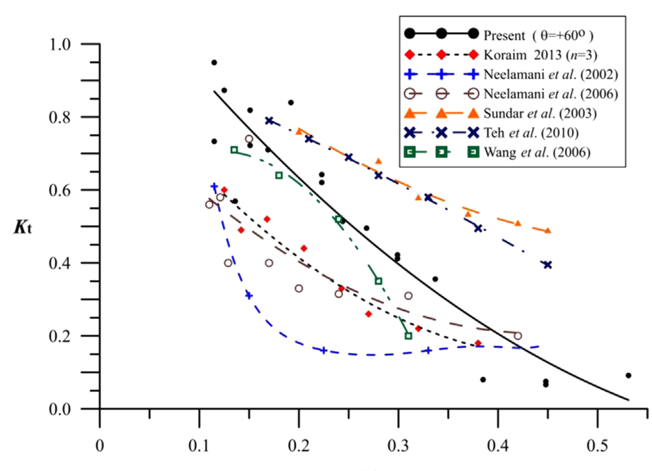

Fig. 19. Comparison of the transmission coefficient K_t between the present highly pervious pipe breakwater (D/h=0.024, w/h=0.4 and $\theta=+60°$) and different models from previous studies (Neelamani and Gayathri, 2006).

breakwater gives lower values of K_r because of the property of highly pervious dense pipes. However, the disadvantage is that the transmission coefficients K_t of short-period waves have good effectiveness, but increased for long-period waves (Fig. 19).

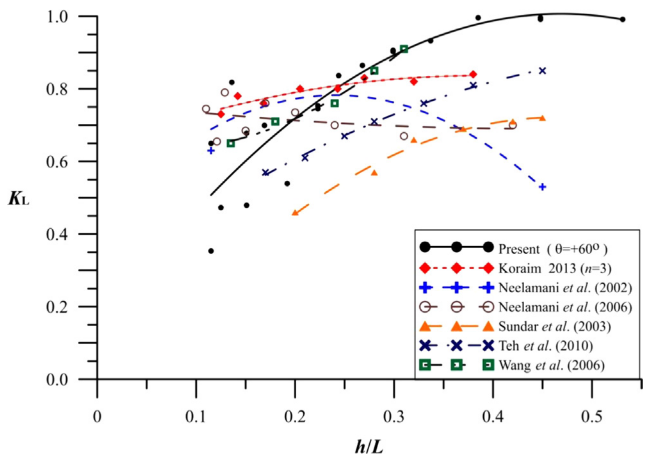

Fig. 20. Comparison of the loss coefficient K_L between the present highly pervious pipe breakwater ($D/h=0.024$, $w/h=0.4$ and $\theta=+60°$) and different models from previous studies (Neelamani and Gayathri, 2006).

Fig. 20 shows that the present breakwater gives higher values of loss coefficient when $h/L>2.5$, and gave a fair performance when $h/L<2.0$.

5. Conclusion

This article presents a distinct highly pervious pipe breakwater constructed from PVC pipes of varying dimensions. Pipe breakwaters were installed at an inclined and highly pervious arrangement, exhibiting high porosity and permeability. The effects of the inclined pipe breakwater were investigated experimentally, and favorable results were obtained. Salient inferences based on the results are as follows:

According to the results of the experiment, the effect of the pipe apertures (was smaller than that of the inclination, and the effect of the inclination was smaller than that of the pipe length. Although the transmission coefficient of $D/h=0.024$, 0.032, 0.040, 0.048 and 0.064 differed, the effects of the varied apertures (decrease 14% transmittance between $D/h=0.024$ and 0.064) did not exceed the effects of pipe length variations (decrease 22.5% transmittance between $w/h=0.2$ and 0.4).

Overall, the reflection was the largest and K_r was highest (increase 125% to $K_r=0.18$ from 0.08) when $\theta=-30°$, and lowest at $+60°$. The transmission coefficient K_t was also largest when $\theta=-30°$, and minimum (decrease 13.8% to $K_r=0.495$ from 0.574) when $\theta=+60°$. Furthermore, the loss coefficient was comparatively greater (average $K_L=0.785$) when $\theta=+60°$ than at all other angles, which indicates that attenuation was most efficient at $\theta=+60°$.

Regarding the attenuation efficacy of the pipe length variations $w/h=0.2$ and 0.4, the variation in K_r, K_t, and K_L affected energy dissipation. The water particle trajectory of the transmission waves resembled an elliptical shape. Therefore, the attenuation effect on wave transmission kinetic energy was greater when using long pipes than when using short pipes.

The results showed that the following parameters, ranked in order of strength, provided substantial energy dissipation in the inclined pipe breakwater: pipe length $w/h>$ inclined angle $\theta>$ pipe diameter D/h. However, a construction involving long pipes does not meet the weight and thickness requirements, and is in violation of the main purpose and expectation of this research. Moreover, the test results of $w/h=0.2$–0.8 (Shih, 2012) showed that $w/h=0.4$ provided a suitable length for energy dissipation.

The inclination angle can be conveniently modulated. The inclination slightly increased the wetter perimeter of the pipe, which increases the energy dissipation effect when the pipes are lengthened, thereby substantially reducing costs. Furthermore, reducing the aperture improved energy dissipation. However, comparisons of the transmission and loss coefficients indicate that small diameters increase substantive attenuation. This experimental investigation of the pore structure of a permeable breakwater device under various conditions established that the inclined pipe breakwater provides optimal energy dissipation when $D/h=0.024$, the inclination angle $\theta=+60°$, and the pipe length $w/h=0.4$.

Coastal structures often partially damaged by the great intensity of impact force of the wave, the effects of wave impacts are one of the important factors on the safety and destructions of coastal structures. Therefore, for the future works, the variation of wave pressure and impact force on the surface of the structure will be measure by water-pressure gauges and digital force gauges, and investigate on the variations and characteristics as well as the effectives on reducing the wave force on highly pervious embankment.

Acknowledgements

The authors wish to express their gratitude for the financial aids of the Ministry of Science and Technology, Republic of China, under Grant no. NSC 102-2221-E-236-002-MY2.

References

Bayram, A., 2000. Experimental study of a sloping float breakwater. Ocean Eng. 27, 445–453.
Bergmann, H., Oumeraci, H., 1998. Wave pressure distribution on permeable vertical walls. In: Proceedings of the 26th International Conference on Coastal Engineering, Copenhagen, Denmark, pp. 2042–2055.
Brossard, J., Jarno-Druaux, A., Marin, F., Tabet-Aoul, E.H., 2003. Fixed absorbing semi-immersed breakwater. Coast. Eng. 49 (1–2), 25–41.
Goda Y., Suzuki Y., 1976. Estimation of incident and reflected waves in random wave experiments. In: Proceedings of the 15th International Conference on Coastal Engineering, Honolulu, pp. 828–845.
Hegde, A.V., Kamath, K., Deepak, J.C., 2008. Mooring forces in horizontal interlaced moored floating pipe breakwater with three layers. Ocean Eng. 35, 165–173.
Hegde, A.V., Kamath, K., Magadum, A.S., 2011. Performance characteristics of horizontal interlaced multilayer moored floating pipe breakwater. J. Waterway, Port, Coast. Ocean Eng., ASCE 133 (4), 275–285.
Huang, Z., 2007. An experimental study of wave scattering by a vertical slotted barrier in the presence of a current. Ocean Eng. 34, 717–723.
Kirkgöz, M.S., 1995. Breaking wave impact on vertical and sloping coastal structures. Ocean Eng. 22, 35–48.
Koftis T., Prinos P., 2005. On the hydrodynamic efficiency of floating breakwaters. In: Proceedings of the 1st International Conf. on Coastal Zone Management and Engineering in the Middle East. Dubai, United Arab Emirates.
Koraim, A.S., 2013. Hydrodynamic efficiency of suspended horizontal rows of half pipes used as a new type breakwater. Ocean Eng. 64, 1–22.
Koraima, A.S., Iskanderb, M.M., Elsayedb, W.R., 2014. Hydrodynamic performance of double rows of piles suspending horizontal c shaped bars. Coast. Eng. 84, 81–96.
Koraim, A.S, Salem, T.N., 2012. The hydrodynamic characteristics of a single suspended row of half pipes under regular waves. Ocean Eng. 50, 1–9.
Liu, C., Huang, Z., Tan, S.K., 2009. Nonlinear scattering of non-breaking waves by a submerged horizontal plate: experiments and simulation. Ocean Eng. 36, 1332–1345.
Mani, J.S., Jayakumar, S., 1995. Wave transmission by suspended pipe breakwater. J. Waterway, Port, Coast. Ocean Eng., ASCE 121 (6), 335–338.
Murakami, H., Itoh, S., Hosoi, Y., Sawamura, Y., 1994. Wave induced flow around submerged sloping plates. In: Proceedings of the 24th Conference Coastal Engineering, 2, ASCE, pp. 1454–1468.
Nakamura, T., Kohno, T., Morita, Y., 2001. Performance of a double-walled barrier with a front wall of inclined plate array. In: Proceedings of the 11th International Offshore and Polar Engineering Conference. Stavanger, Norway, 3, pp. 499–505.
Neelamani, S., Gayathri, T., 2006. Wave interaction with twin plate wave barrier. Ocean Eng. 33, 495–516.
Neelamani, S., Muni Reddy, M.G., 2002. Wave forces on a vertical cylinder defenced by a perforated vertical and inclined barriers. Indian J. Mar. Sci. 31 (3), 179–187.
Neelamani, S., Sandhya, N., 2005. Surface roughness effect of vertical and sloped seawall in incident random wave fields. Ocean Eng. 32, 395–416.

Patil, S.G., Mandal, S., Hegde, A.V., 2014. Performance of a floating pipe breakwater based on intelligent computing. In: Proceedings of the 5th Indian Conference on Harbour and Ocean Engineering, pp. 1 – 6.
Patil, S.G., Mandal, S., Hegde, A.V., Alavandar, Srinivasan, 2011. Neruo-fuzzy based approach for wave transmission prediction of horizontally interlaced multilayer moored floating pipe breakwater. Ocean Eng. 38, 186–196.
Rao, S., Shirlal, K.G., Rao, N.B.S., 2002. Wave transmission and reflection for two rows of perforated hollow piles. Indian J. Mar. Sci. 31, 283–289.
Rao, S., Shirlal, K.G., Varghese, R.V., Govindaraja, K.R., 2009a. Physical model studies on wave transmission of a submerged inclined plate breakwater. Ocean Eng. 36, 1199–1207.
Rao, S., Shirlal, K.G., Varghese, R.V., Prashanth, S., 2009b. Experimental investigation of hydraulic performance of a horizontal plate breakwater. Int. J. Earth Sci. Eng. 2 (5), 424–432.
Reddy, M.S., Neelamani, S., 1992. Wave transmission and reflection characteristics of a partially immersed rigid vertical barrier. Ocean Eng. 19, 313–325.
Shih, R.S., 2012. Experimental study on the performance characteristics of porous perpendicular pipe breakwaters. Ocean Eng. 50, 53–62.
Sundar, V., Anand, K.V., 2010. Dynamic pressure and run-up on curved seawalls compared with vertical wall under cnoidal waves. Indian J. Geo-Mar. Sci. 39 (4), 579–588.
Teh, H. M., Venugopal, V., Bruce, T., 2010. Hydrodynamic performance of a free surface semicircular perforated breakwater. In: Proceedings of the 32nd International Conference on Coastal Engineering, Shanghai, China, pp. 1 – 13.
Teh, H.M., Venugopal, V., Bruce, T., 2012a. Hydrodynamic characteristics of a free surface semicircular breakwater exposed to irregular waves. J. Waterway, Port, Coast. Ocean Eng. 138 (2), 149–163.
Teh, H. M., Venugopal, V., Bruce, T., 2012b. Performance Analysis of composite semicircular breakwaters of different configurations and porosities. In: Proceedings of the 33rd International Conference on Coastal Engineering, Santander, Spain.
Wang, H.Y., Sun, Z.C., 2010a. Experimental study on the influence of geometrical configuration of porous floating breakwater on performance. J. Mar. Sci. Technol. 18 (4), 574–579.
Wang, H.Y., Sun, Z.C., 2010b. Experimental study of a porous floating breakwater. Ocean Eng. 37, 520–527.
Yu, X., 2002. Functional performance of a submerged and essentially horizontal plate for offshore wave control: a review. Coast. Eng. J. 44 (2), 127–147.